

Chapter 2

Kinematic Coupling Design

A fundamental technology of high-precision mechanical interfaces for modular machine and instrumentation structures is the kinematic coupling. This chapter provides a fundamental description of kinematic coupling design, with special considerations given to interfaces used in equipment that is subject to large disturbance forces. While traditional ball-groove kinematic couplings are a century-old design offering micron-level repeatability, developments of recent research have produced variants suited to special high-load, high-cycle, and high-volume installation applications, including the canoe ball coupling [1], the quasi-kinematic coupling [2], the three-tooth coupling [3], and most recently the three-pin coupling. For all such types, closed form relations or well-grounded approximations directly guide interface geometry design and material selection when the load case is known. This chapter presents contact mechanics theory applied to kinematic couplings, and briefly discusses design processes for traditional, canoe ball, quasi-kinematic, and three-pin interfaces.

2.1 Traditional Kinematic Couplings and Fundamental Design Theory

Kinematic couplings have been used for over a century as a method of precisely locating components of a mechanical assembly. The oldest, most common form is the three-ball/three-groove kinematic coupling shown schematically in Figure 2.1. The ball/groove coupling matches a planar, triangular arrangement of three hemispheres on one component to three “vee-grooves” on another component. This match deterministically constrains all six degrees of freedom (DOF) -- three directions of translation and three directions of rotation -- between the components.

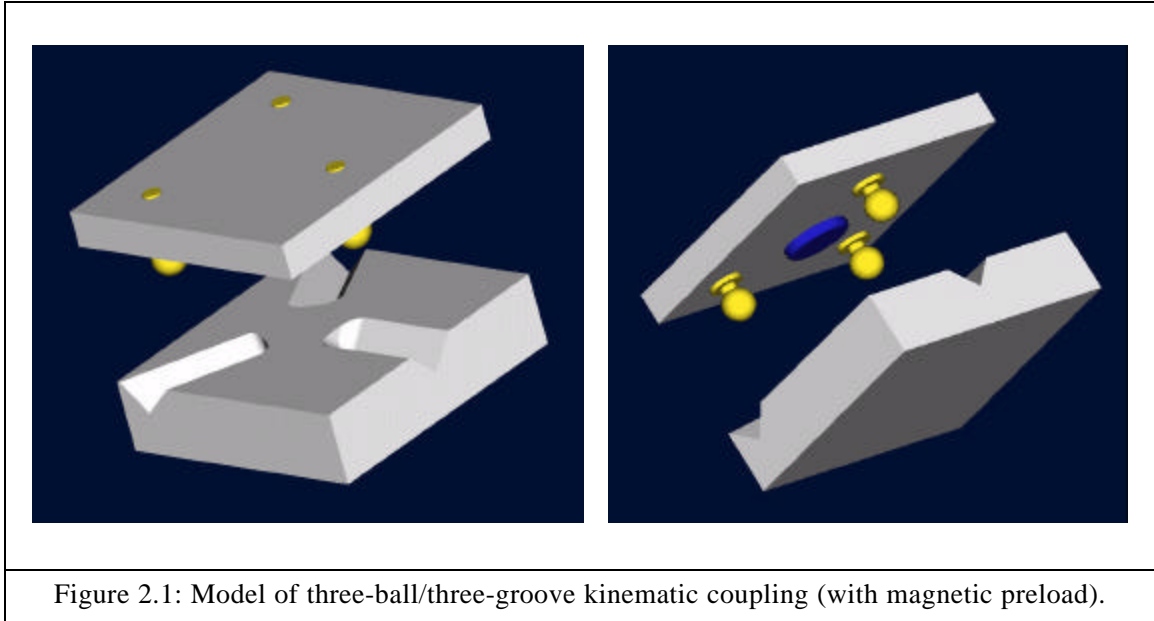


Figure 2.1: Model of three-ball/three-groove kinematic coupling (with magnetic preload).

The stability of a kinematic coupling interface is maximized when the coupling ball and groove centerlines, the normals to the planes containing pairs of contact force vectors, intersect at the centroid of the coupling triangle as shown in Figure 2.2. In other words, the centerlines bisect the angles of the coupling triangle, and intersect at a point called the coupling centroid. For static stability, the planes containing the pairs of contact force vectors must form a triangle [4]. Beyond this, in a specific case of external dynamic loading of the interface, stability is ensured by checking that none of the contact forces reverse from a compressive state, and applying a necessary preload to meet this condition.

Stiffness of a kinematic coupling is also related to the coupling layout. Stiffness is equal in all directions when all the contact force vectors intersect the coupling plane at 45-degree angles. Coupling stiffness can be adjusted by changing the interior angles of the coupling triangle; elongating the triangle in one direction will increase the stiffness about an axis normal to the coupling plane and normal to the direction of elongation, and decrease the stiffness about an axis in the coupling plane and normal to the direction of elongation [4].

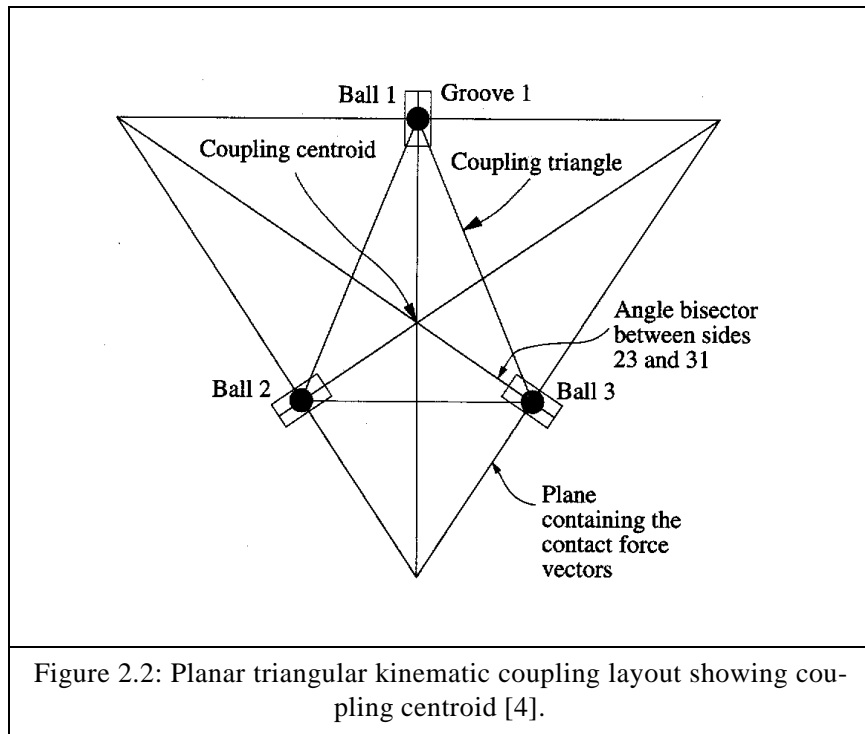


Figure 2.2: Planar triangular kinematic coupling layout showing coupling centroid [4].

Traditionally, kinematic coupling performance is characterized in terms of repeatability versus applied load and the number of interface engagement cycles. Repeatability depends upon several factors including the coupling material and geometry, the preload and the working load, the number of coupling cycles, and the coupling surface finish and its exposure to debris. Hence, repeatability is almost exclusively an experimentally-defined parameter. At high numbers of cycles, fretting corrosion between plain steel surfaces can degrade repeatability; hence, non-corroding materials are best for use in high-cycle applications [4].

Most recently, Hale has presented computational models for predicting repeatability of a coupling interface, parametrized by groove angle and coefficient of friction between the balls and grooves [5]. Maxwell's criterion is applied to determine the sensitive sliding direction for a coupling layout, and the frictional non-repeatability is predicted for when an interface is assembled imperfectly and is stopped short of its nominal seating position by interfacial resistance between the balls and grooves. Maxwell's criterion specifies that each half-groove constraint should be aligned to the direction of motion allowed by the other five constraints, such that in vector notation perfect alignment gives a unit vector inner product of one between the prescribed and constrained sliding directions [6].

For a case study of a simple symmetric ball/groove interface, Hale finds the optimal groove angle to be 58° , with repeatability error at this angle approximately half of that at 30° and 80° [5]. Nonrepeatability (\mathbf{r}) due to friction decreases linearly with decreasing coefficient of friction between the balls and grooves, following the general relation between the friction coefficient (\mathbf{m}) ball radius (R), the applied load (P), and the elastic modulus (E):

$$\rho = \mu \left(\frac{2}{3R} \right)^{\frac{1}{3}} \left(\frac{P}{E} \right)^{\frac{2}{3}}. \quad (2.1)$$

For example, repeatability could be improved by coating polished steel couplings with a low-friction material such as titanium nitride (TiN, $\mathbf{m} = 0.05$), or using a two-layer coating of TiN over tungsten disulfide (WS_2) to increase durability of the coated surface.

For industrial applications, simple ball/groove kinematic couplings can achieve excellent repeatability. For example, repeatability below 2 microns is likely attainable with a hardened steel tooling ball and a non-milled mild steel vee groove. This is more than adequate for most robotic applications. In applications of modular interfaces where parts are interchanged between mounting locations, interface interchangeability is also a critical parameter. Here, the repeatability becomes a random non-deterministic error about the deterministic kinematic error caused by manufacturing variation. Neglecting the mechanical deflections between the balls and grooves, a kinematic transformation model of deterministic coupling interchangeability can easily be built knowing the relative positions of the balls and grooves of the mating interface.

2.1.1 Design Considering Hertzian Contact Stresses

For a deterministically-constrained coupling joint, contact forces, contact stresses, and coupling deflections can be calculated directly from the coupling geometry using known mechanical relations based on Hertzian theory of contact between solid bodies. When considering contact between two curved bodies, a straightforward shortcut is to convert the problem into an equivalent case of contact between a sphere and a flat [7]. From the equivalent major and minor radii of the individual bodies, the equivalent radius of the single sphere is:

$$R_e = \frac{1}{\frac{1}{R_{1,major}} + \frac{1}{R_{1,minor}} + \frac{1}{R_{2,major}} + \frac{1}{R_{2,minor}}} \quad (2.2)$$

Similarly, an equivalent Young's modulus of elasticity between the bodies is defined from the individual moduli (E_1, E_2) and Poisson's ratios (ν_1, ν_2):

$$E_e = \frac{1}{\frac{(1-\nu_1^2)}{E_1} + \frac{(1-\nu_2^2)}{E_2}} \quad (2.3)$$

Then, between a sphere and a flat with R_e and E_e , the radius of an equivalent circular contact area upon application of normal force F is:

$$a = \left(\frac{3FR_e}{2E_e} \right)^{\frac{1}{3}} \quad (2.4)$$

The resultant Hertz contact stress, maximum at the center of the interface, is:

$$q = \frac{1}{\pi} \left(\frac{1}{R_e} \right)^{\frac{2}{3}} \left(\frac{3E_e^2 F}{2} \right)^{\frac{1}{3}} = \frac{aE_e}{\pi R_e} \quad (2.5)$$

Hence, between a sphere and a flat, contact pressure increases with the cube root of applied load. In the separate case of contact of cylinders, the width of the contact region (between a semi-infinite cylinder and a plane, ignoring end effects present with a finite cylinder) and contact pressure increase with the square root of applied load. Here, the half-width of the contact area is:

$$b = \left(\frac{2Fd}{\pi L E_e} \right)^{\frac{1}{2}}, \quad (2.6)$$

where F is the total applied force, L is the length of contact, and d is the cylinder diameter. Then, the maximum contact pressure is:

$$q = \left(\frac{2FE_e}{\pi dL} \right)^{\frac{1}{2}} = \frac{2F}{\pi bL} \quad (2.7)$$

The Hertzian relations assume that significant dimensions of the contact area are small compared with the dimensions of each body and with the relative radii of curvature of the surfaces, and that the surfaces are frictionless so that only a normal pressure is transmitted between them. For kinematic couplings, a rule of thumb in the first case is that the vee-groove flat should allow one diameter of the contact area in non-

contacting space all the way around the deformed region. If the assumptions of Hertzian contact are violated, the contact solution becomes much more complex, involving multidimensional integrals with non-uniform boundary conditions. Coverage of these cases is out of scope of this study; Johnson provides an excellent and comprehensive treatment [7].

Based on the principles of contact mechanics, the static mechanics solution for a traditional kinematic coupling interface is a four step process. Assuming negligible friction at the contacts, calculation of the contact forces is decoupled from calculation of the contact deflections and the gross error motion of the interface. The solution procedure is as follows:

1. Input the interface geometry and the disturbance pattern -- the locations of the contact points in the plane, the groove surface angles, and the magnitudes and locations of the external forces and the preloads -- and solve the six-by-six static equilibrium system to determine the contact forces:

$$AF = B, \quad (2.8)$$

where A is a six-by-six matrix composed of the direction cosines of the groove flats, F is a column vector of the six contact forces, and B is a column vector of the applied disturbance forces and moments.

2. Input the ball and groove major and minor radii, and the ball and groove materials, and then calculate the stresses, deflections, and contact zone sizes of the balls and grooves.
3. Knowing the sizes of the contact zones, verify the applicability of Hertz theory to the contact stress solutions.
4. Assuming small movements, calculate the resulting error motion (HTM) of the interface due to the static deflections at the contact points.

These solutions for ball/groove coupling design were first presented in the convenient format of a spreadsheet in 1986 by Slocum, and in 1992 were revised to include calculations of the static error motions of the interface due to mechanical deflections at the contact points [8,9]. For work of this thesis, the spreadsheet was converted to a MATLAB script. Contrasting the visual format of the spreadsheet, the MATLAB code allows one to specify ranges of parameters and execute iterative design studies (through nested loops) through consecutive runs of the model. The script *kcgen.m* is in Appendix B, and has takes the command line argument *kcgen*. This program can be executed for equal- and non-equal-angle interfaces. All design input parameters are specified within the top section of the code.

2.1.2 Design For Interfaces Under High Dynamic Disturbances

Compared to a design for seating with little or no dynamic disturbance, design of kinematic interfaces for high disturbance loads, with high-cycle applications, requires consideration of interface strength and stability in three areas:

1. **Static performance:** resistance of the coupling to compressive yield in the Hertzian contact zones.
2. **Dynamic performance:** stiffness of the coupling interface and deflections at the point of error measurement upon application of large dynamic forces and torques
3. **Long-term durability:** integrity of the contact surfaces over several million load cycles.

When disturbance forces are applied, the interface design must remain stable at all points within the disturbance space. Considering the disturbance to be a set of three orthogonal forces and three orthogonal moments applied at a central point, stability throughout the disturbance space is guaranteed if stability exists at all limits of the disturbance space. Hence, when the six-tuple is defined in a dynamic application as a set of six upper-bound and lower-bound cycle limits, the linear nature of the force-equilibrium system guarantees that the extreme point will be at one of the sixty-four combinations of the individual force and moment limits.

Considering these principles, in the case of a nominally deterministic interface such as one of traditional or canoe ball couplings, an iterative design procedure is defined:

1. Given the disturbance forces (disturbance space) and interface geometry (coupling positions and groove angles), determine the preload necessary to maintain stability of the interface.
2. Given a nominal material choice, determine the contact surface radius (or radii if desired to be different) necessary to support the superposition of this preload onto the disturbance force space, without causing simple compressive failure in the contact zone.
3. Verify the high-cycle performance of the interface based upon surface and mechanical integrity fatigue-life relations, choosing a different material if necessary. Recalculate the necessary surface radius if desired and re-check for durability.
4. Choose an appropriate fastener to support the tensile preload and tensile disturbance loads, considering static and high-cycle dynamic performance. If the preload is applied through the center of the coupling, appropriately package the fastener through a clearance hole, increasing the size of the contact elements if necessary.

With more design freedom, it is straightforward to extend this process into an iterative optimization; e.g. determining the coupling positions and angles that maximize interface stability and/or minimize the contact stress ratios given the magnitude and breadth of the disturbance load space.

2.2 Canoe Ball Couplings

The main caveat to traditional ball/groove couplings, where the sphere diameters are approximately the widths of the vee grooves to which they mount, is that their near-kinematic nature means that their load capacity is limited to that of the six small near-point contacts. To build greater load capacity yet maintain performance, in 1986 Slocum developed the “canoe ball” shape, which emulates the contact region of a ball as large as 1 m in diameter in an element as small as 25 mm across. A canoe ball mount, shown in Figure 2.3, mates to a standard vee groove, with significantly larger safe contact area than a ball of equivalent diameter that would contact the groove at the same points. The canoe ball shape is achieved by means of precision CNC machining, where the block protrusion with cylindrical shank is first made, then the shank is held in a collet and the spherical surfaces are cylindrically ground by programming the grinding head to move about the virtual central axes of the surfaces. Mullenheld’s initial work showed radial repeatability of 0.1 microns for an equilateral triangle configuration of 250 mm radius stainless steel canoe balls mounted to a 0.2 m diameter solid aluminum test fixture [10].

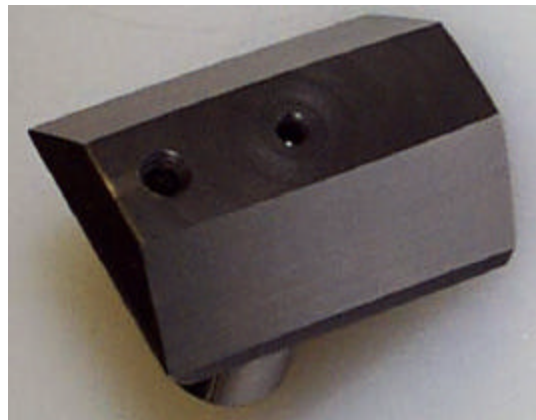


Figure 2.3: Canoe ball mount with 250 mm contact surface radii.

It follows from Hertz theory that if canoe balls with large equivalent radii replace smaller spherical balls, the normal stiffness of the interface will gain by the cube root of the ratio of the contact surface dimensions:

$$G = \left(\frac{R_c}{R_l}\right)^{\frac{1}{3}} \quad (2.9)$$

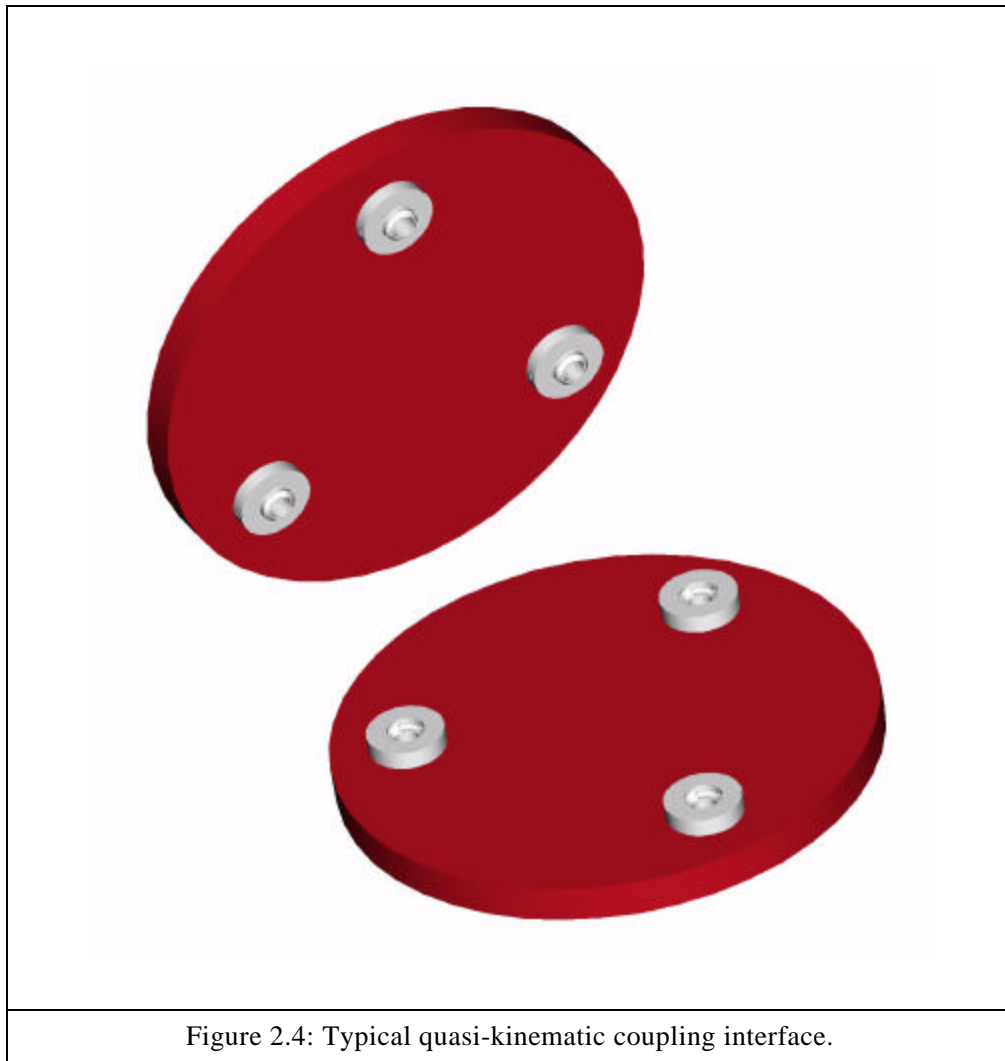
Canoe ball couplings are designed by the same process as traditional ball/groove couplings, only that the input ball radius becomes the large radius of the canoe surfaces, and the contact point locations are defined by specifying the diameter of a sphere that would contact the grooves at the same points as the canoe ball unit.

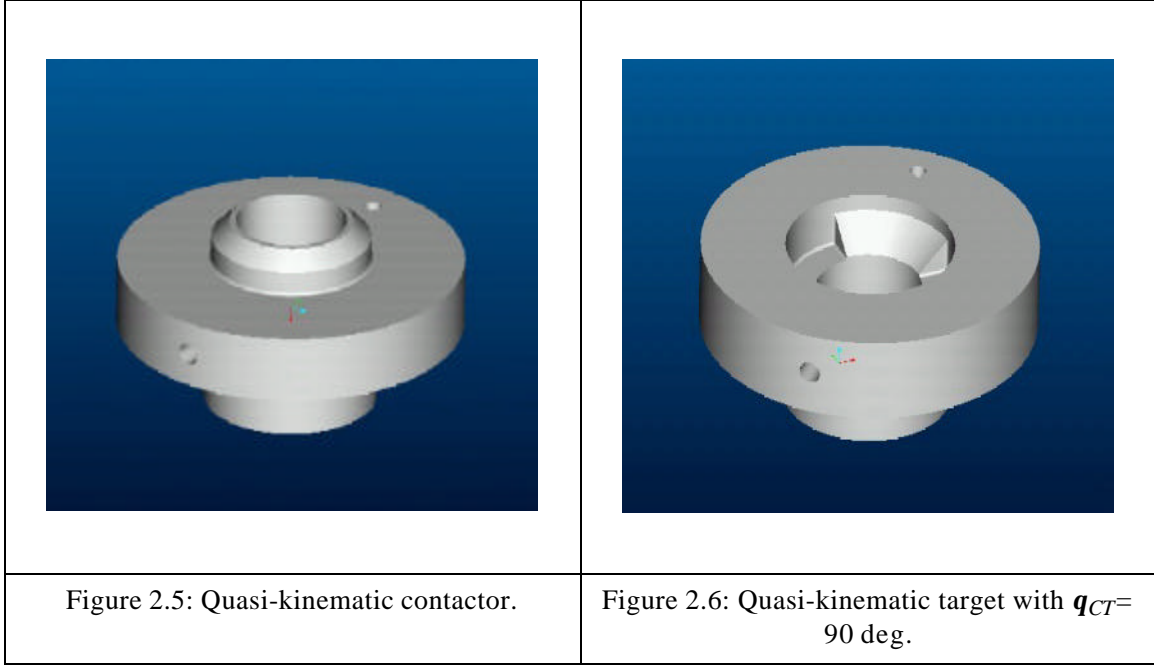
2.3 Quasi-Kinematic Couplings

Compared to the near-exact constraint provided by ball/groove couplings, quasi-kinematic couplings, developed by Culpepper in 2000, create slightly overconstrained attachment using simple, rotationally-symmetric mating units. These cause slight plastic deformation of conical groove surfaces with side reliefs. While quasi-kinematic couplings sacrifice accuracy from ball/groove interfaces, the simple geometry reduces cost and enables direct machining of the coupling halves into mating components. Exploiting this cost vs. accuracy trade-off makes quasi-kinematic coupling well-suited to high-volume precision manufacturing applications.

Figure 2.4 shows a typical quasi-kinematic coupling, with the male halves called *contactors*, and the female halves called *targets*. Based on the contact angle q_{CT} , each contactor engages in line contact of length $2pD_Cq_{CT}$ with the corresponding target, where D_C is the diameter of the contact circle. Quasi-kinematic interfaces are typically designed such that a static gap exists between the normal contact surfaces of the interface halves when the contactors and targets first touch, and then a preload is applied to seat the interface and close the gap. The preload serves to seek the nominal interface seating position by overcoming contact friction and by brinelling away surface inconsistencies at the contact areas. The deformation of the contactors and targets when the preload is applied may be fully elastic, or it may be partially elastic and partially plastic. In the latter case, only part of the static gap is recovered when the interface is unloaded, and the contactors and/or the targets are permanently deformed (based on choice of same or different

strength materials) and create a sort of “surface memory” for re-seating the interface. Hence, when the gap is closed the large mating horizontal surfaces, not the quasi-kinematic line contacts, dictate the normal stiffness. This high normal stiffness is desirable for high-load bearing machine applications. This design precludes kinematic interchangeability, but for many applications -- such as Culpepper’s case study of repeatably mounting the same engine block to its bedplate during subsequent manufacturing operations -- this design is acceptable.





Because of the arc-shaped line contact of quasi-kinematic couplings, the exact force-equilibrium solution is non-deterministic. To give a good approximation of the exact solution, first displacements are imposed to determine the normal contact stiffnesses, then the forces are calculated. In the case of elastic-plastic contact, nonlinear behavior due to plastic flow dictates the use of finite element analysis (FEA) to estimate a power-law force-deflection relationship for usage in the analytical stiffness relations. For FEA simulation of contact problems, Culpepper showed that the mesh size of contacting elements should be no larger than 5% the width of the contact region.

Presentation of the exact force-deflection relationship for the spherical target and conical contactor are beyond the scope of this thesis; however, based on an initial design geometry, straightforward calculations show the boundary between elastic and plastic deformation of the contacts. The force per unit length (f_{nYIELD}) at which plastic flow begins is:

$$f_{nYIELD} = \frac{2.8\pi R_e \sigma_y}{E_e}, \quad (2.10)$$

where R_e and E_e are the equivalent radius and modulus of the contact, calculated in the traditional Hertzian fashion. Now the contact displacement that induces plastic flow is known from:

$$\delta_n = \left(\frac{f_n}{\pi}\right) \left\{ \frac{(1-v_1^2)}{E_1} \left(2 \ln \left(2R_1 \left(\left(\frac{\pi E_e}{R_e f_n} \right)^{\frac{1}{2}} - 1 \right) \right) \right) + \frac{(1-v_2^2)}{E_2} \left(2 \ln \left(2R_2 \left(\left(\frac{\pi E_e}{R_e f_n} \right)^{\frac{1}{2}} - 1 \right) \right) \right) \right\}. \quad (2.11)$$

By simple trigonometry, the corresponding displacement in the z-direction is:

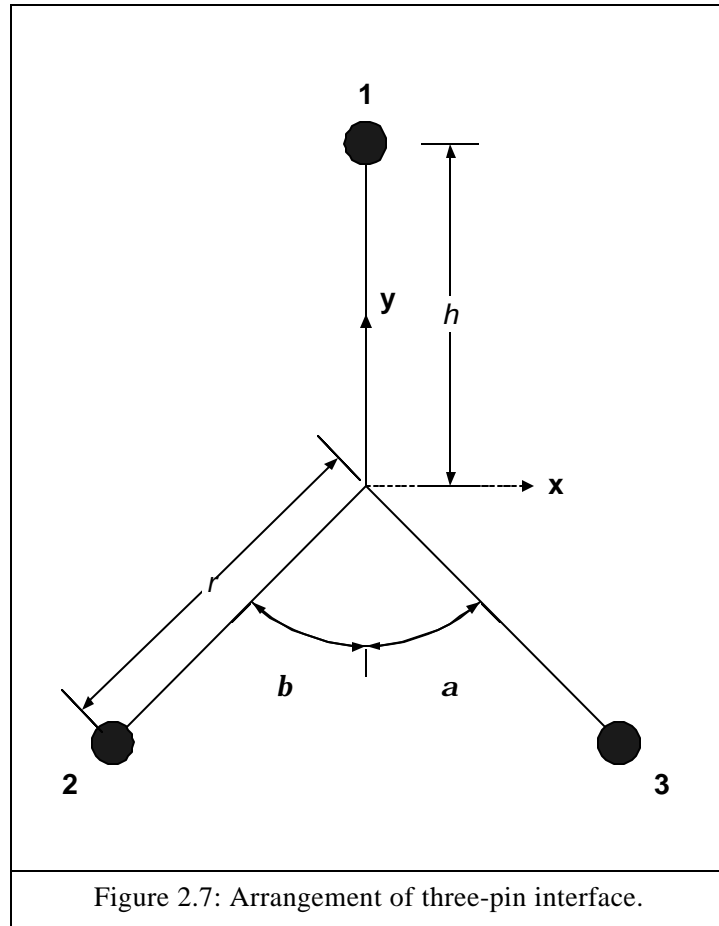
$$\delta_z = \frac{\delta_n}{\sin(\theta_c)}. \quad (2.12)$$

These relations can be used after determining the initial input geometry to qualitatively estimate the magnitude of elastic and plastic contact, and given suitable dimensional tolerances for the gap size, to estimate how manufacturing variation affects the type of deformation at the contacts. With a full force-deflection model, one can calculate the necessary preload to close the gap, and the appropriate gap size and preload necessary to maintain stability under the dynamic loads can be calculated. The contactor radii and target contact angle can be chosen to give the appropriate gap dimension, in-plane stiffness (magnitude and direction coupled), and normal stiffness for closure.

Culpepper [11] gives a thorough explanation of modeling, analysis, design, and manufacture of quasi-kinematic couplings.

2.4 Three-Pin In-Plane Coupling

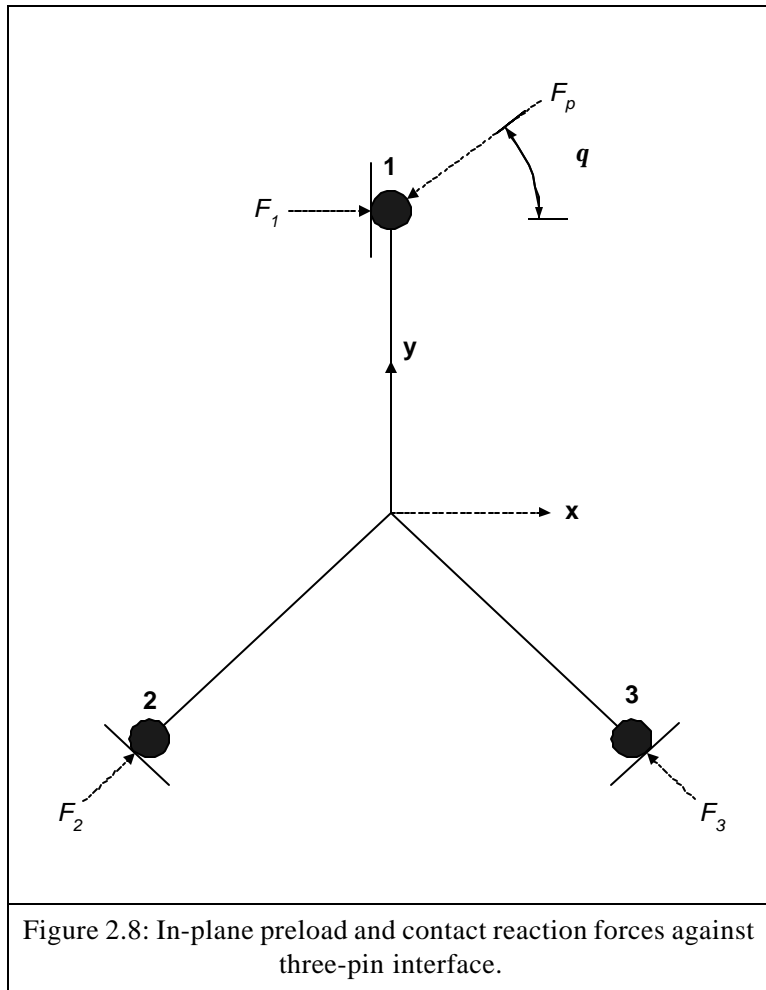
The three-pin coupling is a second type of quasi-kinematic coupling. The three-pin coupling establishes near-exact constraint in the horizontal plane using three pins resting on curved control surfaces perpendicular to the horizontal plane of constraint, and maintains remaining control from normal preload forces against large horizontal contact forces in the plane. The three-pin interface is shown schematically in Figure 2.7, where the first pin lies along the local y-axis at offset h from the frame origin, and the second and third pins are offset by distance r from the origin and angles \mathbf{a} and \mathbf{b} from the y-axis.

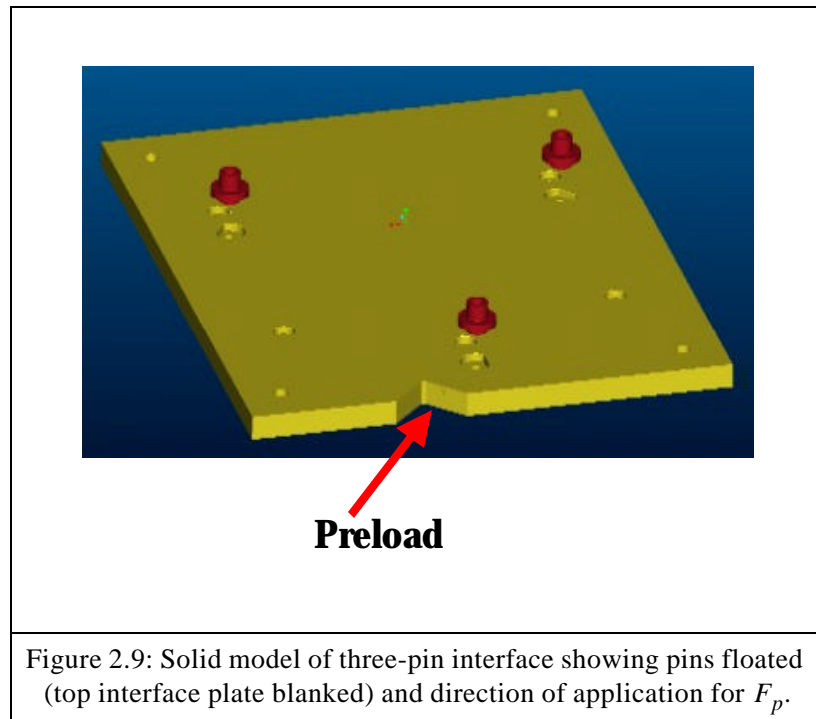


The three-pin interface is realized by fashioning an upper interface plate with a triangular arrangement of shouldered or dowel pins, and manufacturing a bottom interface with a triangular arrangement of oversized cutouts with flat or curved contact surfaces with which the pins make contact. When the top interface plate is engaged with the bottom interface plate, the pins are seated against the contact surfaces by introducing an in-plane preload force (F_p) at the first pin, offset by the angle θ from the local x-axis. A disturbance load $D_o = [D_{x,o}, D_{y,o}, D_{z,o}, DM_{x,o}, DM_{y,o}, DM_{z,o}]$ is resolved into an effective six-tuple $D = [D_x, D_y, D_z, DM_x, DM_y, DM_z]$ applied at the local origin, and normal preload forces F_{z1} , F_{z2} , and F_{z3} are applied using bolts through the centers of pins 1, 2, and 3, respectively. Assuming normal reaction forces at each of the engagement locations between the pins and bottom plate, the in-plane reaction forces and the required normal preloads to maintain dynamic stability are the solution of the static system:

$$\begin{bmatrix} F_1 \\ F_2 \\ F_3 \\ F_{z1} \\ F_{z2} \\ F_{z3} \end{bmatrix} = \begin{bmatrix} 1 & \sin(\alpha) & -\sin(\beta) & 0 & 0 & 0 \\ 0 & \cos(\alpha) & \cos(\beta) & 0 & 0 & 0 \\ 0 & 0 & 0 & 1 & 1 & 1 \\ 0 & 0 & 0 & -r\cos(\alpha) & -r\cos(\beta) & h \\ 0 & 0 & 0 & -r\sin(\alpha) & -r\sin(\beta) & 0 \\ h & 0 & 0 & 0 & 0 & 0 \end{bmatrix}^{-1} \begin{bmatrix} D_x - F_p \cos(\theta) \\ D_y - F_p \cos(\theta) \\ D_z \\ DM_x \\ DM_y \\ DM_z + F_p h \cos(\theta) \end{bmatrix} \quad (2.13)$$

When the pins are engaged to the bottom interface plate and F_p is applied to seat the pins against the contact surfaces, the static reaction forces are those obtained from (2.13) with $D = 0$, hence requiring no vertical preload to maintain stability.





The process of seating the pins against the contact surfaces by applying the in-plane preload involves relative sliding of the horizontal contact surfaces (e.g. pin shoulders) between the top interface assembly and the bottom plate. Before all three pins are in their rest positions, relative sliding of the horizontal contact surfaces, plus relative sliding of one or two pins that may already be in contact, generates frictional resistance against the preload. Hence, the maximum preload needed to seat all three pins properly is the maximum frictional resistance generated among the multiple cases of:

1. No pins in contact.
2. Pin 1 only in contact.
3. Pin 2 only in contact.
4. Pin 3 only in contact.
5. Pins 1 and 2 in contact.
6. Pins 1 and 3 in contact.
7. Pins 2 and 3 in contact.

Cases 3 and 4 result in motion combining rotation of the top interface assembly about the axis of pin in

contact, and translation of the assembly along the line dictated by the contact surface. Here, sub-cases of pure rotation about the pin and pure translation along the contact surface line give the worst-case resistance. Cases 5, 6, and 7, can be considered as rotations of the top assembly about the instant centers determined by the pair of sliding directions of the pins in contact. Denoting the static vertical load on the interface (e.g. weight of the machine module) as F_z , and the static coefficient friction between the horizontal surfaces as μ the minimum preload needed to overcome case 1 is simply:

$$F_{p1} = \mu F_z. \quad (2.14)$$

For case 2, the minimum preload when the interface slides about pin 1 is given by:

$$F_{p2} = \frac{\mu F_z}{\sin(\theta) - \mu \cos(\theta)}, \quad (2.15)$$

where θ is the in-plane application of F_p , measured relative to the line through the preloaded pin and the coupling centroid. This methodology can be straightforwardly extended, balancing the frictional resistances against the preload and contact forces, in the remaining cases and subcases (3a, 3b, 4a, and 4b for pure rotation and pure translation respectively for each case). Then, the required in-plane preload is formally:

$$F_p = \max[F_{p1}, F_{p2}, F_{p3a}, F_{p3b}, F_{p4a}, F_{p4b}, F_{p5}, F_{p6}, F_{p7}] \quad (2.16)$$

When a bolt is used to apply the load, only a small torque (e.g. 20 N-m) is needed to seat an interface with that bears a relatively large normal load (e.g. 25 kN). To ensure repeatable seating under variation in the preload and surface conditions, a safety factor of 1.5 or 2 is suggested beyond the minimum required preload.

The force balance of (2.13) assumes an ideal case of three-point contact, one in which the contact forces between the pins and the bottom interface load must provide all the necessary in-plane resistance to counteract the disturbance forces. However, since the contacts are lines rather than points, and frictional resistance exists between the horizontal and vertical mates, the necessary resistance after the preload is applied is taken primarily by friction between the contact surfaces. Hence, the vertical preloads calculated from (2.13) are necessary to ensure stability, yet an in-plane preload force not much larger than that required to deterministically seat the pins is needed. To satisfy this assumption, a second model must be

built to show that the frictional resistance between the horizontal contacts, subject to the vertical preloads, is sufficient to prevent slippage when only the required preload for interface seating is applied in the plane. Then the pins can be sized appropriately by limiting the Hertzian line contact stresses experienced from contact with the bottom plate, using the cylinder-line contact relations presented in Section 2.1.1.

The calculations of (2.3) and of all cases of frictional resistance against interface seating are handled by the MATLAB scripts *threepins.m* and *threepins_friction.m*, given in Appendix B. Interface geometry and disturbance force parameters are specified directly in the files.

In summary, the major design process steps for the three-pin interface are:

1. Define the nominal interface geometry, placing the pins and contact surfaces relative to a central reference.
2. Determine the in-plane preload needed to seat the interface in the horizontal plane, based on the static normal load.
3. Determine the vertical preload needed at each pin to maintain dynamic stability of the interface.
4. Apply a factor of safety over the in-plane contact forces dictated by (2), and size the pins appropriately to avoid yield along the line contacts.

2.5 Fatigue Life Considerations

When kinematic couplings are designed for high-cycle applications involving oscillating contact stresses, attention to the long-term durability of the contacting materials is necessary. Quantitatively, the contact stresses can be related to the applied loads through Buckingham's load stress factor (K) to predict the onset of mechanical breakdown of the surfaces. This factor is similar to the factor K_g used in endurance evaluation of gear teeth through extensive periods of cycling Hertzian contact. S_{fe} , the surface endurance strength, gives the maximum sustainable contact stress to keep onset of fatigue from happening before a specified number of cycles. For contact between a cylinder and a flat, the relation is:

$$K = \frac{2Fd}{L} = \frac{\pi S_{fe}^2}{E_e} \quad (2.17)$$

For contact between a generalized sphere and a flat, the relation is:

$$K = \left(\frac{3F}{2}\right)^{\frac{1}{2}} \left(\frac{1}{R_e}\right) = \frac{(\pi S_{fe})^{\frac{3}{2}}}{E_e}. \quad (2.18)$$

Relations between S_{fe} and the number of load cycles are well-known for many materials; for example, at 10^7 cycles, the allowable contact stress, in kpsi, for steel alloys is related to the Brinell hardness (H_B) by:

$$\sigma = 0.364 H_B + 27 \text{ kpsi} \quad (2.19)$$

For between 10^7 and 10^{10} cycles, the allowable contact stress is related to H_B and the number of cycles (N) by:

$$\sigma = 2.46 N^{-0.056} (0.364 H_B + 27) \text{ kpsi} \quad (2.20)$$

Table 2.1 gives representative fatigue strengths and ratios to nominal yield strength (s_y) for two selected steel alloys at varying numbers of cycles. For example, AISI 1018 steel can withstand full contact loading to its yield strength for 10^7 and 10^9 cycles, yet the endurance limit drops far below the yield limit 10^{10} cycles. For AISI 420 stainless, the reduction occurs just before 10^9 cycles.

Material	H_B (Rockwell)	N	s [kpsi]	s/s_y
AISI 1018 (as rolled)	126 (B71)	10^7	72.7	1.34
AISI 1018 (as rolled)	126 (B71)	10^9	56.2	1.04
AISI 1018 (as rolled)	126 (B71)	10^{10}	49.4	0.91
AISI 420 Stainless	594 (C67)	10^7	242.6	1.23
AISI 420 Stainless	594 (C67)	10^9	187.5	0.95
AISI 420 Stainless	594 (C67)	10^{10}	164.7	0.83

Table 2.1: Fatigue strengths of selected steel alloys [12].

2.6 Interface Packaging and Tightening Torque Specification

Finally, along with designing the couplings to meet the life-cycle stress demands of an application, consideration must be made to packaging of the couplings on a machine interface, and if necessary to appropriate selection of bolts to apply the preload. In general, couplings should be placed near the outer-

most constraints of the interface, and the holding plate should be designed to limit undesirable mechanical deflections or modal behavior under application of the dynamic loads. Bolts can be placed directly through the coupling centers or directly outboard of the contacts. In either case, applying a higher bolt preload than needed for stability will only enhance stiffness and stability, so the maximum preload within the stress limit of the desired fastener and the Hertz stress allowance for the contacts can be used. Here, one can initially solve the six-by-six equilibrium force system to determine the necessary preloads to maintain stability, then iterate to higher preloads until the Hertz stress limit, considering an appropriate factory of safety, is met.

In terms of the applied torque (Γ), the bolt lead (l , $1/l$ threads per unit length), the efficiency (e), the bolt diameter (D_B), and the coefficient of friction (μ) under the bolt head, the axial force in the bolt is [13]:

$$F = \frac{4\pi\Gamma}{\frac{2l}{e} + 3\pi D_B \mu} . \quad (2.21)$$

When the required axial force is selected in coupling design, this relation gives the required tightening torque.

Shigley [13] and Slocum [4] provide thorough references on bolted joint design.

